Microstructure dependence of fatigue crack propagation behavior in wrought magnesium alloy

S. Morita, S. Fujiwara, T. Hori, N. Hattori
Department of Mechanical Engineering, Saga University, 1 Honjo, Saga 840-8502, Japan
morita@me.saga-u.ac.jp

H. Somekawa
National Institute of Materials Science,
SOMEKAWA.Hidetoshi@nims.go.jp

T. Mayama
Kumamoto University,
mayama@kumamoto-u.ac.jp

ABSTRACT. This paper deals with the fatigue crack propagation behavior of rolled AZ31B magnesium alloy (grain size: approximately 40 μm). Fatigue crack propagation tests were performed on single edge notched tension specimens at a stress ratio of R = 0.1 and a frequency of 10 Hz at room temperature. Loading axes were parallel to the rolling direction; fatigue cracks propagated parallel to the transverse direction (L-T specimen), parallel to the short transverse direction (L-S specimen). Loading axis was perpendicular to the rolling direction; fatigue cracks propagated parallel to the transverse direction (S-T specimen). The crack growth rate (da/dN) of the L-S specimen was several times lower than that of the L-T specimen in the examined stress intensity factor range (ΔK). Fracture surfaces of the L-T and L-S specimens showed many steps parallel and perpendicular, respectively, to the macroscopic crack growth direction. The da/dN of the S-T specimen was higher than that of the L-T and L-S specimens in the examined ΔK. The fracture surface was covered by quasi-cleavage facets independent of macroscopic crack growth direction, and the fracture surface roughness at low ΔK was larger than that at high ΔK.

KEYWORDS. Fatigue crack; Texture; Magnesium.

INTRODUCTION

Magnesium alloys are the lightest structural material with high specific strength and stiffness. These features make magnesium alloys attractive for applications in the automotive industry [1]. Wrought Mg-Al-Zn system alloys, especially rolled and extruded magnesium alloys, are the candidates for structural parts. It is necessary to investigate the fatigue crack initiation and propagation behavior of the material used for structural parts.

It is well known that magnesium alloys have a hexagonal close-packed (HCP) structure, and strong textures are formed by rolling. In such textured magnesium alloys, basal planes are aligned parallel to the rolling direction by rolling. Depending on their texture, rolled magnesium alloys show unique deformation behavior such as mechanical anisotropy [2-4], pseudoelasticity in cyclic loading-unloading [4-8], and asymmetricity of stress-strain hysteresis loops in strain controlled low-cycle fatigue tests [9-14] and even in load controlled high-cycle fatigue tests [3, 9], etc. The orientation dependence of fatigue crack propagation behavior of magnesium single crystals [15-17], and the effect of grain size [18-21] and texture [22-25] on fatigue properties of polycrystalline magnesium alloys have been reported in previous works. However, the effect of texture on the fatigue crack propagation behavior of magnesium alloy is still poorly understood. In the present study, the crystallographic orientation dependence of the fatigue crack propagation behavior of rolled AZ31B magnesium alloy is investigated.

EXPERIMENTAL PROCEDURE

Commercial rolled AZ31B magnesium alloy plate with a thickness of 60 mm was used in the present study. Chemical composition of the alloy is listed in Tab. 1. The alloy has equiaxed grains, and the average grain size was approximately 40 μm. The alloy showed typical texture as shown in Fig.1 and Fig.2; basal planes were aligned parallel to the rolling direction. Three types of tensile and compressive specimens were machined with the loading axis parallel (L-specimen), perpendicular (T-specimen) and normal (S-specimen) to rolling direction. Compressive and tensile mechanical properties of the alloy is summarized in Tab. 2.

Al	Zn	Mn	Fe	Si	Cu	Ni	Mg
3.1	0.929	0.41	0.003	0.037	0.004	0.001	Bal.

Table 1: Chemical composition. (mass%)

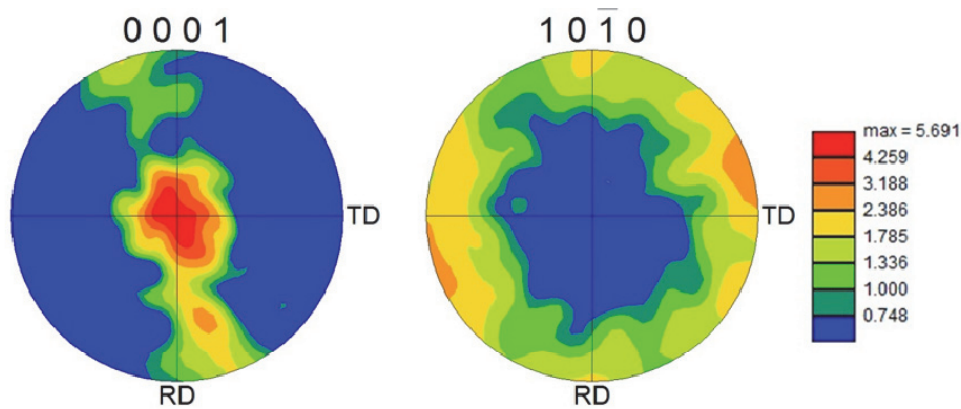| Specimen	Compressive 0.2% proof stress, $\sigma_{0.2comp}$ [MPa]	Tensile 0.2% proof stress, $\sigma_{0.2tens}$ [MPa]	Tensile strength, σ_B [MPa]	Tensile fracture strain, El [%]
L-specimen	78	129	240	10
T-specimen	73	94	240	12
S-specimen	85	53	255	15

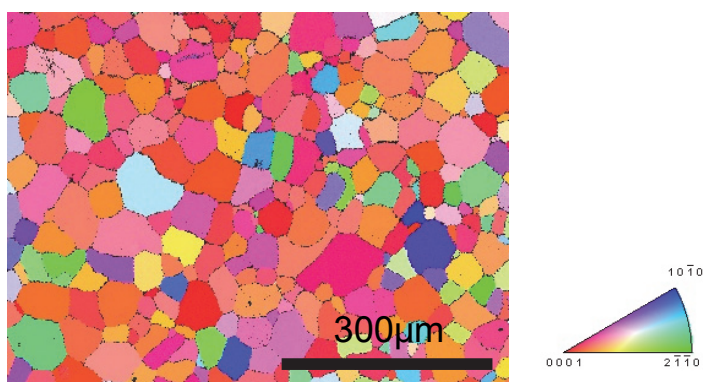Table 2: Mechanical properties.

Figure 1: (0001) and (10-10) pole figures.

Figure 2: IPF map.

Single edge notched tension specimens with a width (*W*) of 12 mm, a thickness (*B*) of 4 mm, a initial crack length (*a*) of 1 mm, and a length (*L*) of 50 mm were machined from a rolled as shown in Fig.3. Loading axes were parallel to the rolling direction; fatigue crack propagated parallel to the transverse direction (L-T specimen), parallel to the short transverse direction (L-S specimen). On the other hand, loading axis was normal to the rolling direction; fatigue cracks propagated parallel to the transverse direction (S-T specimen). Fatigue crack propagation tests were performed on an electro-hydraulic testing machine (capacity: 9.8 kN) at a stress ratio of $R = P_{min}/P_{max} = 0.1$ (tension-tension) and a frequency of 10 Hz at room temperature in air. Here, P_{max} and P_{min} are the maximum and minimum applied load, respectively. The fatigue crack length was determined using a microscope. The stress intensity factor range (*ΔK*) was calculated using the following equation:

$$\Delta K = \frac{\Delta P}{B\sqrt{W}} \cdot \frac{\sqrt{2\tan\frac{\pi a}{2W}}}{\left(\cos\frac{\pi a}{2W}\right)} \left[0.752 + 2.02\left(\frac{a}{W}\right) + 0.37\left(1 - \sin\frac{\pi a}{2W}\right)^3 \right] \tag{1}$$

where *P* is the applied load, and *W*, *B* and *a* are the width, thickness, and crack length, respectively.
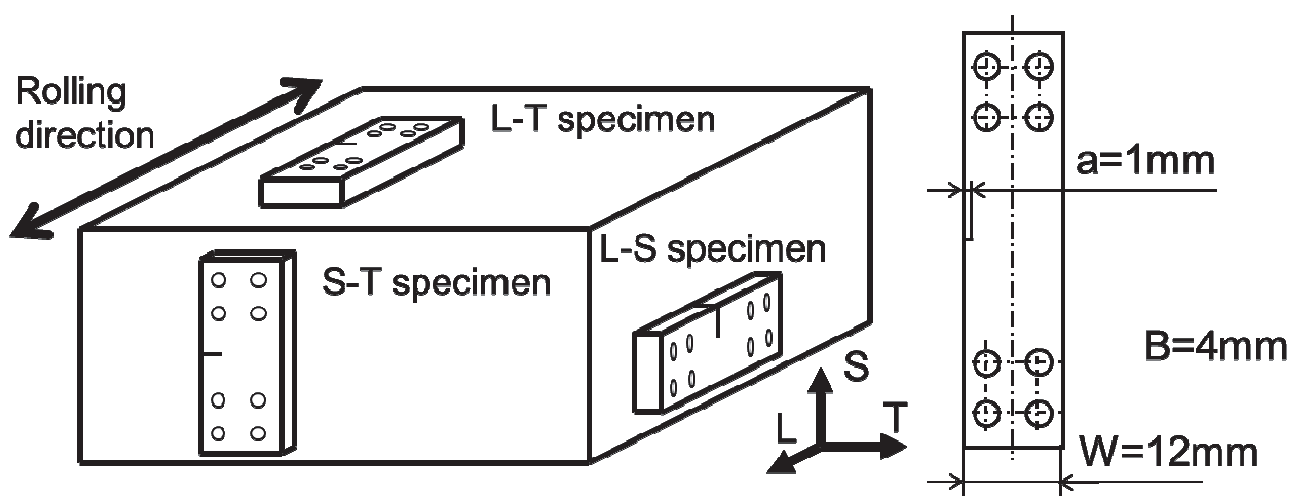The fracture surface of the fatigue tested specimens were observed by SEM.

Figure 3: Shape and dimensions of SENT specimen (in mm).

RESULTS AND DISCUSSION

The relationship between the crack growth rate (da/dN) and the ΔK is shown in Fig.4. The figure shows that the da/dN of the L-S specimen was several times lower than that of the L-T and S-T specimens in the examined ΔK. The da/dN of the S-T specimen was higher than that of the L-T and L-S specimens in the examined ΔK.

Fig. 5 shows the typical SEM images of the fatigue tested L-T, L-S, and S-T specimens. Many straight lines or steps were observed over several grains along with the macroscopic direction of fatigue crack growth in the L-T specimen (Fig.5(a) and (b)). In contrast, in the L-S specimen, many lines or steps perpendicular to the macroscopic direction of fatigue crack growth were observed (Fig.5(c) and (d)). The fracture surface of the L-T and L-S specimens had a similar morphology and did not depend on ΔK. On the other hand, various quasi-cleavage facets independent of the macroscopic direction of fatigue crack growth were observed in the S-T specimen (Figs.5(e) and (f)). Moreover, the fracture surface roughness at low ΔK, up to $\Delta K = 7$ MPa·m$^{1/2}$, was larger than that at high ΔK, above $\Delta K > 7$ MPa·m$^{1/2}$.

The macroscopic fatigue crack propagation is parallel to the *a*-axis (perpendicular to basal plane) of each grain for the L-T specimen, and parallel to the *c*-axis (perpendicular to basal plane) of each grain for the L-S specimen. Therefore, it is inferred that the *c*-axis direction is unfavorable for the fatigue crack propagation in rolled AZ31B magnesium alloy. It is also found that the macroscopic fatigue crack propagation is various directions to the *a*-axis (parallel to basal plane) of each grain in the S-T specimen. Thus, it appears that the fatigue crack propagated easily in a direction parallel to the *a*-axis (parallel to basal plane) of each grain in the S-T specimen.

In addition, the deformation twinning of polycrystalline magnesium alloys plays an important role in the deformation process because of the limitation of slip system. When the specimens were subjected to a stress higher than the compressive and tensile yield stress in the load-controlled fatigue test, deformation twins were observed in the extruded magnesium alloys [3, 4, 26]. In contrast, free deformation twins are observed around the fatigue crack path (within the plastic zone) in the L-T and L-S specimens. It appears that the fatigue crack growth is not controlled by the deformation twinning at a crack tip in textured polycrystalline magnesium alloys.
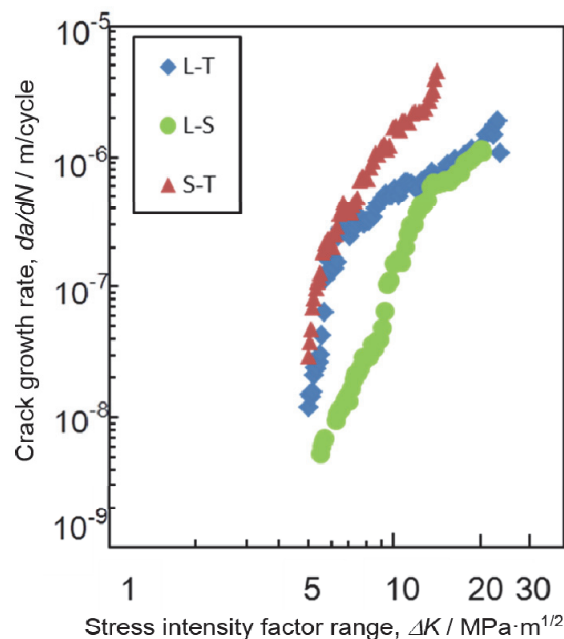

Figure 4: Relationship between crack growth rate and stress intensity factor range.

CONCLUSIONS

The fatigue crack propagation behaviors of three types of specimens of textured polycrystalline magnesium alloy, in which the macroscopic fatigue crack propagated perpendicular to and parallel to the basal plane of each grain, has been investigated. It is found that the *a*-axis direction is favorable for the fatigue crack propagation in textured
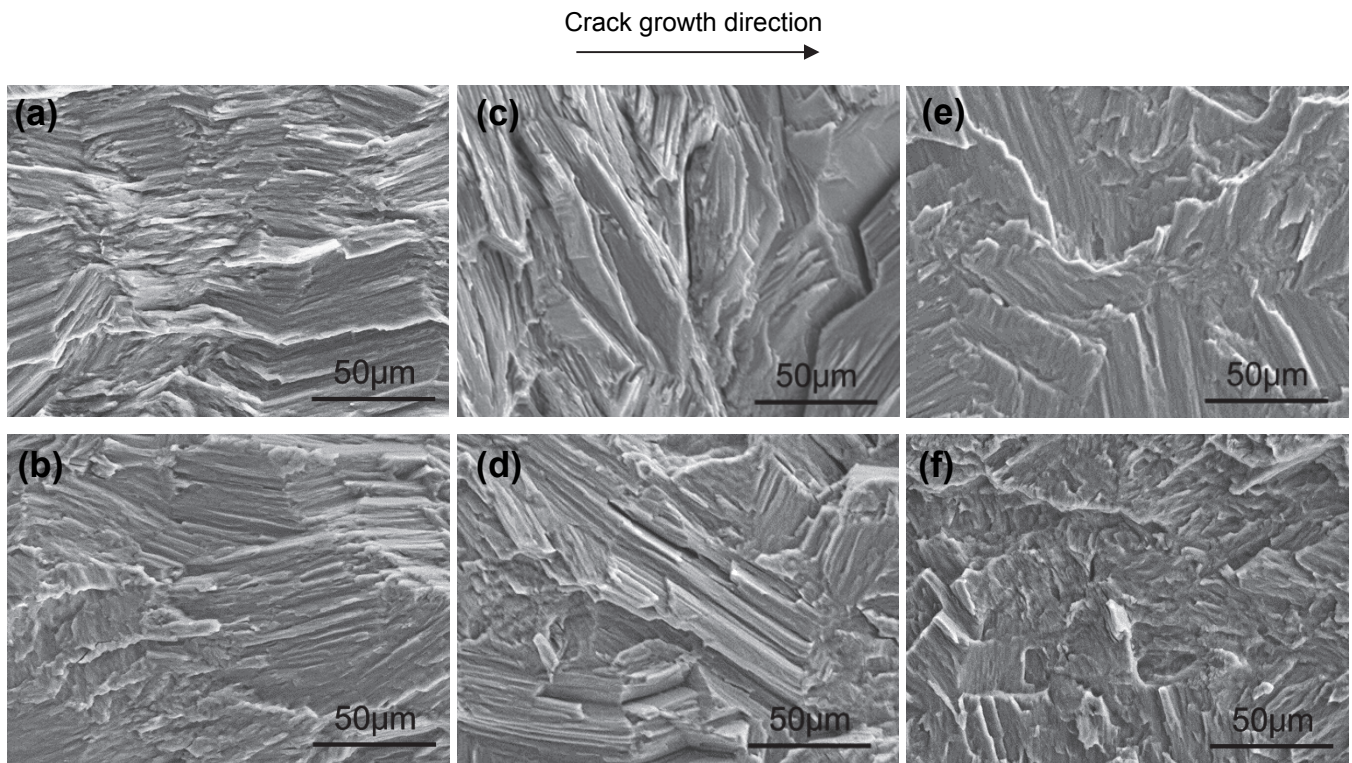
polycrystalline magnesium alloy.

Crack growth direction

Figure 5: Fracture surfaces of fatigue tested (a) L-T specimen at ΔK = 6.8 MPa·m$^{1/2}$, da/dN = 10^{-7} m/cycle; (b) L-T specimen at ΔK = 13 MPa·m$^{1/2}$, da/dN = 10^{-6} m/cycle; (c) L-S specimen at ΔK = 6.4 MPa·m$^{1/2}$, da/dN = 10^{-8} m/cycle; (d) L-S specimen at ΔK = 13 MPa·m$^{1/2}$, da/dN = 10^{-6} m/cycle; (e) S-T specimen at ΔK = 6.2 MPa·m$^{1/2}$, da/dN = 10^{-7} m/cycle; and (f) S-T specimen at ΔK = 7 MPa·m$^{1/2}$, da/dN = 10^{-6} m/cycle.

REFERENCES

[1] Ebert, T., Mordike, B.L., Magnesium Properties – applications – potential, Mater. Sci. Eng. A, 302 (2001) 37–45.
[2] Yukutake, E., Kaneko, J., Sugamata, M., Anisotropy and Non-Uniformity in Plastic Behavior of AZ31 Magnesium Alloy Plates, Mater. Trans., 44 (2003) 452–457.
[3] Somekawa, H., Maruyama, N., Hiromoto, S., Yamamoto, A., Mukai, T., Fatigue Behaviors and Microstructures in an Extruded Mg-Al-Zn Alloy, Mater. Trans., 49 (2008) 681–684.
[4] Morita, S., Tanaka, S., Ohno, N., Kawakami, Y., Enjoji, T., Cyclic deformation and fatigue crack behavior of extruded AZ31B magnesium alloy, Mater. Sci. Forum, 638-642 (2010) 3056–3061.
[5] Cáceres, C.H., Sumitomo, T., Veridt, M., Pseudoelastic behaviour of cast magnesium AZ91 alloy under cyclic loading–unloading, Acta Mater., 51 (2003) 6211–6218.
[6] Li, Y., Enoki, M., Evaluation of the Twinning Behavior of Polycrystalline Magnesium at Room Temperature by Acoustic Emission, Mater. Trans., 48 (2007) 1215–1220.

[7] Li, Y., Enoki, M., Deformation and anelastic recovery of pure magnesium and AZ31B alloy investigated by AE, Mater. Trans., 48 (2007) 2343–2348.

[8] Li, Y., and Enoki, M., Recovery Behaviour of Pure Magnesium in Cyclic Compression-Quick Unloading-Recovery Process at Room Temperature Investigated by AE, Mater. Trans., 49 (2008) 1800–1805.

[9] Hasegawa, S., Tuchida, Y., Yano, H., Matsui, M., Evaluation of low cycle fatigue life in AZ31 magnesium alloy, Int. J. Fatigue, 26 (2007) 1839–1845.

[10] Lin, X.Z., Chen, D.L., Strain controlled cyclic deformation behavior of an extruded magnesium alloy, Mater. Sci. Eng. A, 496 (2008) 106–113.

[11] Matsuzuki, M., Horibe, S., Analysis of fatigue damage process in magnesium alloy AZ31, Mater. Sci. Eng. A, 504 (2009) 169–74.

[12] Begum, S., Chen, D.L., Xu, S., Luo, Alan A., Effect of strain ratio and strain rate on low cycle fatigue behavior of AZ31 wrought magnesium alloy, Mater. Sci. Eng. A, 517 (2009) 334–343.

[13] Lv, F., Yang, F., Duan, Q.Q., Luo, T.J., Yang, Y.S., Li, S.X., Zhang, Z.F., Tensile and low-cycle fatigue properties of Mg–2.8% Al–1.1% Zn–0.4% Mn alloy along the transverse and rolling directions, Scripta Mater., 61 (2009) 887–890.

[14] Park, S.H., Hong, S.G., Bang, W., Lee, C.S., Effect of anisotropy on the low-cycle fatigue behavior of rolled AZ31 magnesium alloy, Mater. Sci. Eng. A, 527 (2010) 417–423.

[15] Ando, S., Iwamoto, N., Hori, T., Tonda, H., Fatigue Crack Propagation in Magnesium Crystals, J. Japan Inst. Metals, 65 (2001) 187–190.

[16] Ando, S., Saruwatari, K., Hori, T., Tonda, H., Fatigue Crack Propagation Behavior in Magnesium Single Crystals, J. Japan Inst. Metals, 67 (2003) 247–251.

[17] Ando, S., Ikejiri, Y., Iida, N., Tsushida, M., Tonda, H., Orientation Dependence of Fatigue Crack Propagation in Magnesium Single Crystals, J. Japan Inst. Metals, 70 (2006) 634–637.

[18] Kim, H.-K., Lee, Y.-I., Chung, C.-S., Fatigue properties of a fine-grained magnesium alloy produced by equal channel angular pressing, Scripta Mater., 52 (2005) 473–477.

[19] Uematsu, Y., Tokaji, K., Kamakura, M., Uchida, K., Shibata, H., Bekku, N., Effect of extrusion conditions on grain refinement and fatigue behaviour in magnesium alloys, Mater. Sci. Eng. A, 434 (2006) 131–140.

[20] Ochi, Y., Masaki, K., Hirasawa, T., Wu, X., Matsumura, T., Takigawa, Y., Higashi, K., High Cycle Fatigue Property and Micro Crack Propagation Behavior in Extruded AZ31 Magnesium Alloys, Mater. Trans., 47 (2006) 989–994.

[21] Tsushida, M., Shikada, K., kitahara, H., Ando, S., Tonoda, H., Relationship between Fatigue Strength and Grain Size in AZ31 Magnesium Alloys, Mater. Trans., 49 (2008) 1157–1161.

[22] Sajuri, Z.B., Miyashita, Y., Hosokai, Y., Mutoh, Y., Effects of Mn content and texture on fatigue properties of as-cast and extruded AZ61 magnesium alloys, Int. J. Mech. Sci., 48 (2006) 198–209.

[23] Ishihara, S., Nan, Z., Goshima, T., Effect of Microstructure on Fatigue Behavior of AZ31 Magnesium Alloy, Mater. Sci. Eng. A, 468-470 (2007) 214–222.

[24] Zeng, R.C., Xu, Y.B., Ke, W., Han, E.H., Fatigue crack propagation behavior of as-extruded magnesium alloy AZ80, Mater. Sci. Eng. A, 509 (2009) 1–7.

[25] Zeng, R., Han, E., Ke, W., Dietzel, W., Kainer, K.U., Atrens, A., Influence of microstructure on tensile properties and fatigue crack growth in extruded magnesium alloy AM60, Int. J. Fatigue, 32 (2010) 411–419.

[26] Yang, F., Yin, S.M., Li, S.X., Zhang, Z.F., Crack initiation mechanism of extruded AZ31 magnesium alloy in the very high cycle fatigue regime, Mater. Sci. Eng. A, 491 (2008) 131–136.